



# DIAGONAL TENSION TESTING OF AS-BUILT AND FABRIC REINFORCED CEMENTITIOUS MATRIX STRENGTHENED MASONRY PANELS

N. Ismail<sup>(1)</sup>, T. El-Maaddawy<sup>(2)</sup>, A. Najmal<sup>(3)</sup> and N. Khattak<sup>(4)</sup>

<sup>(1)</sup> Assistant Professor, Civil and Environmental Engineering Department, United Arab Emirates University, najif@uaeu.ac.ae

<sup>(2)</sup> Associate Professor, Civil and Environmental Engineering Department, United Arab Emirates University, tamer.maaddawy@uaeu.ac.ae

<sup>(3)</sup> Graduate Student, Civil and Environmental Engineering Department, United Arab Emirates University, 201470422@uaeu.ac.ae

<sup>(4)</sup> Research Assistant, Civil and Environmental Engineering Department, United Arab Emirates University, nouman@uaeu.ac.ae

## Abstract

Reinforced concrete frames with infill masonry panels (IMPs) exhibit complex in-plane seismic behaviour, with IMPs contributing to the frame strength/stiffness while acting as shear bracing panels and undergoing damage. Amongst several options, one option to limit such earthquake damage to IMPs is the surface application of a polymer fabric-reinforced cementitious matrix (FRCM). Presented in this article are preliminary results from the first series of tests undertaken as part of an experimental program investigating the effectiveness of FRCM as a strengthening solution to limit shear damage in IMPs. The experimental program involved characterisation of constituent materials (i.e. testing of masonry units, masonry mortar, FRCM matrix) and the diagonal shear testing of as-built and FRCM strengthened test panels. A total of seven test panels were constructed using 150 mm thick hollow concrete masonry units, laid in a stack bond pattern with a 1:3 by mass cement-sand mortar. Experimental results of tested panels were analysed to evaluate their shear stress-strain response, ultimate shear strength, pseudo-ductility, and stiffness characteristics. The experimental results from FRCM strengthened test panels were then compared to those from as-built tested panel to quantify the performance improvement achieved using FRCM strengthening. The shear strength of FRCM strengthened test panels was 180-270% of that from corresponding as-built tested panel, whereas the failure mode changed from brittle collapse to a ductile gradual failure. Typical damage patterns observed in FRCM strengthened test panels included crushing at loaded corners and distributed narrow cracking along the loaded diagonal of the test panel.

*Keywords: diagonal tension; fabric; masonry; infill; strengthening; earthquake.*

## 1. Introduction

Experiences of the past moderate to severe earthquakes suggest that infill masonry panels (IMPs) typically used in reinforced concrete moment frame buildings markedly contribute to the seismic resistant of these buildings and in doing so the IMPs undergo some form of damage or result in damage at infill-frame interface [1-3]. Such IMP damage often result in disruption to building operation albeit to these being structurally sound in many cases. Leaving human loss aside, the cost of strengthening to limit such earthquake damage to IMPs is usually a fraction of the total cost that may arise due to disruption, demolition, and reconstruction of the building after an earthquake [4]. Additionally, cultural and/or historical value associated to these earthquake prone buildings makes the seismic retrofit a preferred choice over reconstruction. The effect of IMPs however is mostly positive on overall strength and stiffness of the building but the increasing rigour for damage avoidance design in structural earthquake engineering profession also demands to limit earthquake damaged to IMPs in design level earthquakes. To this end, substantial research effort had been invested over the last three decades to develop/improve strengthening techniques for the seismic upgrade of existing IMF buildings. Consequently, a community has developed an ever increasing interest to use fibre reinforced polymers (FRP) in strengthening applications. FRP has been used in a variety of forms in seismic strengthening applications, with few examples of conventional FRP strengthening techniques to include epoxy bonded and mechanically fastened FRP plates, near surface mounted strips in cut slits, and surface lay-up of FRP sheets using organic epoxies.



Amongst several advantages of FRP are large strength to weight ratio, simplicity of application, and their availability in different forms such as pre-cured laminates, sheets, grids, and bars. Whilst FRP sheet overlay shows exceptional promise, there still exist few challenges associated with this strengthening technique. These challenges include performance at elevated temperature [5] and in aggressive environment, adhesion to uneven substrate, stiffness incompatibility with softer substrates, and vapour impermeability. The majority of these problems are associated with the organic nature of epoxy used in these conventional FRP applications. Research suggests that the mechanical strength of organic epoxy deteriorates notably at temperatures exceeding the glass transition temperature, which typically ranges from 60°C to 82°C for typical organic epoxy based resins [6]. One option to overcome these challenges is to use FRP grids/fabrics with inorganic cementitious matrices, which is typically referred to as fabric reinforced cementitious matrices (FRCM). FRCM has been experimentally verified to perform satisfactorily at much higher temperature than the glass transition temperature of FRP [7].

Some key benefits of FRCM systems have also been listed in ACI 549.4-13 [8], which include its inherent heat resistance, compatibility with masonry and concrete substrates, ability to be applied to curved and un-even surfaces, vapour permeability, and resistance to water and alkali attack. In FRCM applications, grid pattern FRP fabrics sandwiched between thin (typically 2-4 mm) layers of inorganic cementitious matrix are bonded onto substrate surface receiving the strengthening application. In technical literature, FRCM has also been referred to as textile reinforced mortar (TRM) or fibre reinforced grid (FRG) system. Key objective of the experimental program presented herein was to appraise the potential of this relatively new strengthening technique to limit earthquake damage to IMPs by increasing their strength and deformation capacity, which would also avoid the damage to surrounding frame that could result from brittle shear failure of masonry panels along a single bed joint.

## 2. Precedent Experimental Studies

### 2.1 Testing of FRCM strengthened IMFs and masonry walls

Koutas et al. [9] performed quasi-static in plane testing of as built and FRCM strengthened 2/3 scale single bay three-storey high seismic-deficient masonry infilled reinforced concrete frames (IMFs). Three different types of FRCM systems were used, being carbon FRCM, basalt FRCM, and glass FRCM. Test results suggested that the strengthening application improved global seismic response of IMFs both in terms of lateral strength and deformation capacity, with about 56% increase in the lateral strength and 52% increase in deformation capacity when compared to their counterpart as-built tested IMF. Da Porto et al. [10] investigated the performance of IMFs subjected to concurrent out of plane and in plane lateral loading, by testing a total of eight full-scale one-bay and one-storey high IMFs with brick IMP. Glass and basalt based FRCMs were used for strengthening, which were reported to minimally increase the initial stiffness and in plane capacity of tested IMFs. Selim et al. [11] undertook pseudo-static cyclic testing of three one third scale FRCM strengthened IMFs and reported that the strengthened IMFs failed at 66 % larger force amplitudes when compared to test results from the as-built tested IMF.

Kolsch [12] investigated the effectiveness of carbon FRCM to strengthen unreinforced masonry (URM) walls by undertaking out of plane testing of full scale URM walls ( $3 \times 3 \times 0.24 \text{ m}^3$ ) reported FRCM as a viable option to avoid partial or complete out of plane collapse of URM walls. Papanicolaou et al. [13] and Harajli et al. [14] tested small scale URM walls strengthened using glass based FRCM in induced out of plane flexural failure mode under static and cyclic loading. The studies reported FRCM to increase flexural strength, deformation capacity, and ductility of URM walls. Papanicolaou et al. [15] tested URM walls strengthened using both epoxy bonded FRP sheets and glass based FRCM by applying cyclic in plane and out of plane loading and reported FRCM to perform better than epoxy bonded FRP sheets. The minimum out of plane strength increase due to FRCM strengthening noted was 400%, with 130% increase in deformation capacity. FRCM was found to result in 15–30% higher strength than FRP sheets. Babaeidarabad et al. [16] reported carbon FRCM strengthening to increase the out of plane flexural strength of one way spanning URM walls by 1.8-6.5 times their as-built strength.



Table 1 – Review of diagonal tension tests of FRCC strengthened URM/UCM panels

Reference	Wall panel properties				N	FRCC system			% increase in strength	Failure mode
	Masonry material	H (mm)	B (mm)	t (mm)		Fabric material	No. of faces	No. of layers		
Mantagezza [17]	URM	467	467	105	11	C	1/2	1/2	33-281	DC/DB
Yardim and Lalaj [18]	URM	1200	1200	250	12	G	1/2	1	163-300	DC/DB
Ismail and Ingham [19]	URM	1200	1200	220	12	G	1/2	1	14-381	OD/RT
Almeida et al. [20]	CeBM	990	990	190	06	C	2	1	73-230	DC/DB
Babaeidarabad et al. [21]	UCM	1220	1220	92	09	C	2	1/4	195-236	DC/TC
Babaeidarabad et al. [22]	URM	1145	1220	92	09	C	2	1/4	240-473	DC/FS/TC
Basili et al. [23]	TSM	1000	1000	250	06	B	1/2	1	32-54	DC
Faella et al. [24]	TBM	1200	1200	400	09	C	2	1	445-600	DC/DB/S
Parisi et al. [25]	TSM	1230	1230	310	09	G	1/2	1	190-310	RT/OD/S
De Lorenzis et al. [26]	CSM	461	461	100	10	C	1/2	1	84	DC/S
Koutas et al. [27]	UCM	800	800	55	13	C/G/B	1	1/2	54-118	DC

Where: URM= solid clay brick masonry; UCM= hollow concrete block masonry; CeBM= ceramic brick masonry; TSM= tuff stone masonry; CSM=calcareous stone masonry; TBM= tuff brick masonry; H= test panel height; B= test panel length; t= thickness of test panel; N= total number of panels tested; C= CFRP; G= GFRP; B= Basalt; DC= diagonal cracking; TC= toe crushing; S= sliding; DB= de-bonding of FRCC from substrate; FS= fabric slippage inside FRCC i.e. failure at fabric matrix interface; OD= out of plane deformation; and RT= rupture of fabric.

Bernat et al. [28] tested 11 full scale URM walls strengthened using glass and carbon FRCC systems (both one and two layers applied onto both faces) under eccentric compressive load and reported an increase of nearly 100% in the load carrying capacity of FRCC strengthened test walls. Valluzzi et al. [29] tested two FRCC strengthened URM wall using a four-point monotonic face loading. The strength of FRCC strengthened test walls was observed to be seven to eight times the strength of as-built tested URM walls. Bernat-Maso et al. [30] evaluated the flexural strength of small scale URM walls (each being 280×132×560 mm<sup>3</sup>) strengthened by applying FRCC manually and by spraying. Three point out of plane bending tests were performed on a total of 19 URM assemblages, of which 18 were strengthened with three different types of FRCC systems. The FRCC systems differed in terms of fibre makeup (i.e. CFRP, GFRP, steel and basalt) and the type of matrix used. Test results showed a remarkable increase in flexural strength of URM assemblages strengthened using FRCC, which was in the order of 2-6 times the strength of as-built tested wall. Ismail and Ingham [31] reported full scale reversed cyclic in plane testing of three URM pier-spandrel assemblages and out of plane testing of three slender URM walls. The in plane and out of plane strength of FRCC strengthened test walls were 128-136% and 575-786% of that from corresponding as-built tested URM assemblage/wall, respectively. It was also noted that the FRCC strengthening notably increased the deformation and ductility capacity as well and changed the nature of failure from brittle to ductile.

### 2.2 Diagonal shear testing of FRCC strengthened masonry panels

A summary of precedent studies involving diagonal compression testing of FRCC strengthened URM panels is given in Table 1. Faella et al. [24] undertook diagonal shear testing of nine URM panels constructed using yellow coloured tuff masonry bricks strengthened using carbon based FRCC. Diagonal shear strength of FRCC strengthened test panels was observed to range between four and six times the strength of as-built tested URM panels. Babaeidarabad et al. [22] tested a total of nine URM panels strengthened using carbon based FRCC in induced diagonal shear failure mode. Two FRCC strengthening schemes were used, namely one and four layers applied onto both faces. The shear strength of FRCC strengthened test panels with one layer FRCC and four layer FRCC was observed to be 2.4 and 4.7 times the strength of the as-built tested URM panel, respectively. It was concluded that FRCC strengthening is an effective solution to increase stiffness and pseudo-ductility of IMPs. Babaeidarabad et al. [21] investigated the in plane shear strength of nine unreinforced concrete masonry (UCM) panels strengthened using the same one layer and four layer FRCC applications. FRCC strengthened panels exhibited a shear strength of 2.0-2.4 times that of the corresponding as-built tested panel. Ismail and Ingham [19] investigated diagonal shear behaviour of in plane loaded URM walls retrofitted using two type of



FRCM systems (applied on one face and both faces of test panels) by subjecting a total of 12 two leaf thick vintage URM panels (two as built and 10 FRCM retrofitted) to diagonal shear testing, each being  $1.2 \times 1.2 \text{ m}^2$  in size. The test results showed that the increase in diagonal shear strength due to FRCM strengthening ranged from 14% to 48% for one layer FRCM application on one face, whereas one layer FRCM on both faces resulted in a shear strength increase of 346-381%. However, it was noted that the reported in plane strength increase corresponded to a limit state when testing was stopped due to excessive out of plane tilting. Almeida et al. [20] studied effectiveness of carbon FRCM to strengthen shear critical URM wall panels and reported a shear strength increment of 230%, with failure resulting due to delamination of FRCM layer. The delamination of FRCM overlay suggested that, in some cases, use of a transverse connecting system or anchors offer a vital role to fully utilize the strength of FRCM overlay. Yardim and Lalaj [18] tested 12 URM panels with different strengthening techniques including glass FRCM applied on one side of test walls, FRCM application on both sides of test walls, polypropylene based FRCM and ferrocement application under diagonal compression test. Single face FRCM strengthened test walls exhibited the worst performance and underwent out of plane deformation causing large cracks developed on unstrengthened URM face, the failure type reported being similar to Ismail et al. [24]. Test walls with two-face FRCM application showed lower increase in shear modulus.

### 3. Experimental Program

A testing program was undertaken to investigate structural performance of IMPs seismically strengthened using FRCM in an induced diagonal shear failure mode. Seven hollow concrete masonry wall panels were tested in study reported herein, of these one was tested as-built and the remaining six were strengthened with three different types of FRCM systems prior to testing (typically in sets of two receiving the same FRCM strengthening). Testing was continued until either the post-peak shear stress degraded to 80% of the maximum recorded shear strength, or lateral drift reached 1% (about 15 mm displacement).





#### 3.1 Material Properties

As the first step in this study typical masonry types used in the Gulf region were identified and representative sample from each masonry unit was sourced. The masonry types were selected based on the results of a desktop study to review the existing prevailing construction practices in the Gulf region, which included review of building drawings and interviewing design and construction engineers. The masonry types prevalent in the Gulf region include fired clay brick masonry laid in common bond pattern with weak mortar (UBM), different sized hollow concrete masonry units laid in stack bond pattern with cement/sand mortar (CM1 and CM2), and insulated concrete masonry units laid in stack bond pattern using cement/sand mortar (IBM). Mortar compressive strength was determined by testing mortar cubes ( $50 \text{ mm}^3$  in size) in accordance with ASTM C109-08 [32] and the compressive strength of masonry units was determined in accordance with ASTM C270-03 [33], typically in sets of five.

Mechanical properties of each prevalent masonry type were determined experimentally and have been reported in Table 2, as arithmetic mean values with associated percentage coefficient of variation (COV) within the braces. The 150 mm thick hollow concrete masonry units are the most commonly used masonry type in seismic deficient building in the United Arab Emirate (UAE) and thus to imitate typical IMPs prevalent in seismic deficient buildings, all masonry test panels were constructed using the hollow 150 mm thick concrete block masonry. The concrete masonry units were  $400 \times 200 \times 150 \text{ mm}^3$  in size, with a void to block cross sectional area ratio of 0.50. A cementitious mortar with cement:sand ratio (by volume) of 1:3 was used to construct the panel following a stack bond pattern. Quantity of water in mortar mixes was controlled by a skilled mason to keep the mortar to a workable consistency, being similar to typically adopted construction practices. Three different types of FRCM systems were used to strengthen the test panels, with each FRCM system consisting of a FRP fabric and cementitious matrix. The type of fabrics used herein included glass fibre reinforced polymer (GFRP), carbon fibre reinforced polymer (CFRP) and basalt. The cementitious matrix used derives strength from hydration of cementitious and pozzolonic materials, which was reinforced using polyvinyl fibres to allow thicker application. Typically, three 50 mm cubes were casted for each batch of prepared FRCM matrix, which were later tested for compression strength.



Table 2 – Properties of brick/block units and masonry

Masonry type	Concrete masonry- 1	Concrete masonry- 2	Insulated concrete masonry	Burnt clay brick masonry
				
$L_b$ (mm)	400	400	400	240
$W_b$ (mm)	150	200	200	100
$H_b$ (mm)	200	200	200	55
V (%)	50	-	-	50
$f'_b$ (MPa)	7.0 (2.2)	6.8 (1.1)	7.4 (1.0)	7.1 (6.0)
$f'_j$ (MPa)	2.9 (2.1)	2.9 (2.9)	2.9 (2.9)	1.5 (3.4)
$f'_m$ (MPa)*	3.52	3.48	3.6	2.9
E (MPa) <sup>^</sup>	3168	3132	3240	2030

Where:  $L_b$  = typical length of masonry brick/block;  $W_b$  = typical width of masonry brick/block;  $H_b$  = typical height of masonry brick/block; V = percentage void area in masonry brick/block;  $f'_b$  = experimental brick/block compressive strength with %COV within braces; COV = coefficient of variation;  $f'_j$  = mortar compressive strength with %COV within braces;  $f'_m$  = estimated masonry compressive strength; and E = estimated masonry modulus of elasticity. <sup>^</sup>E=700x $f'_m$  for clay masonry and 900x $f'_m$  for concrete masonry [34]; \*calculated by formula:  $f'_m = K f'_b{}^\alpha f'_j{}^\beta$ , where  $\alpha=0.7$ ,  $\beta=0.3$  and K=0.45 for clay masonry and 0.55 for concrete masonry [35].

Table 3 – Indicative physical characteristics of polymer fabrics used in FRCM

FRCM component	GFRP fabric	Basalt fabric	CFRP fabric
MS (mm)	30x30	6x6	30x30
D (g/m <sup>2</sup> )	420	250	≥170
$\rho$ (g/cm <sup>3</sup> )	2.5	2.75	1.83
t (mm)	2	0.039	0.048
$f_t$ (kN/m)	105	60	>240
$\epsilon_u$ (%)	4	1.8	2
$E_f$ (GPa)	32	89	252
$f'_{cj}$ (MPa)	40 (4.9)	38.5 (5.5)	50.9 (0.7)

Where: MS = mesh size; D= density in g/m<sup>2</sup>;  $\rho$ = density of fibre; t= thickness of rovings/fabric;  $f_t$ = tensile strength of fibre grid per running meter;  $\epsilon_u$ = rupture strain of the fibres;  $E_f$ = modulus of elasticity of fibre; and  $f'_{cj}$  = compressive strength of FRCM matrix with %COV within braces.

Experimentally determined compressive strength of FRCM matrices are reported in Table 3 along with indicative physical characteristics of other FRCM materials based on technical literature provided by the manufacturer of the FRCM system used herein.

### 3.2 Test panels details

Test panels were given the notation WAN or WSN, where M refers to wall, A refers to as-built specimens, S refers to fabric type used to strengthen the test panel (G, B, or C), and N denotes the test number. Actual measured test panel dimensions and applied FRCM strengthening details are shown in Table 4, while the masonry bond pattern used is shown in Fig. 1. All test panels were left for 28 days and FRCM were left for at least 14 days for curing prior to testing.

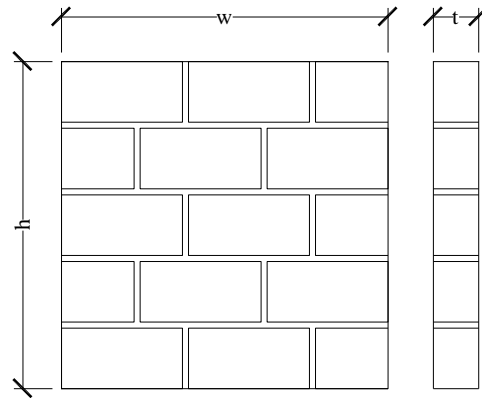


Fig. 1 - Test panel geometry and bond patterns

Table 4 – Test panel dimensions and retrofit details

Test No	Test panel	Test panel dimensions			FRCM strengthening details		
		w (mm)	h (mm)	t (mm)	Thickness (mm)	Polymer fabric type	No. of layers
1	WA1	1045	1070	150	-	-	-
2	WG2	1050	1040	170	10	GFRP	1
3	WB3	1050	1040	168	8	Basalt	1
4	WB4	1070	1040	168	9	Basalt	1
5	WG5	1070	1040	170	10	GFRP	1
6	WC6	1060	1040	170	9	CFRP	1
7	WC7	1075	1060	170	9	CFRP	1

Where: w = wallette length; h = wallette height; t = total wallette thickness (including strengthened materials); GFRP = glass fibre reinforced polymer; CFRP = carbon fibre reinforced polymer.

### 3.3 Strengthening Procedure

The FRCM application was started by cleaning the substrate masonry surface thoroughly by removing dust and fragments, which was then brought to saturated surface dry condition by sprinkling water onto it. The FRCM matrix was prepared using manufacturer instructions by thoroughly mixing the pre-weighed and packed solids and liquid components in a bucket using a mixing attachment with an electric drill machine set to rotary action only (see Fig. 2a). This prepared matrix was applied onto the full face of test panels receiving FRCM strengthening in a thin layer of roughly 3 mm using moderate pressure on levelling trowel (Fig. 2b).

Once the first layer of FRCM matrix has been applied onto the substrate masonry surface, later polymer/basalt mesh cut to exact sizes were placed onto still fresh first layer of FRCM matrix and pressed into the mortar layer using a hand trowel (Fig. 2c). The horizontal rovings of polymer fabric/grid were placed parallel to bed joints and were overlain by a second 3-4 mm thick layer of FRCM matrix hand applied using a trowel. The total thickness of the applied FRCM overlay was kept to approximately 10 mm for all FRCM strengthened test panels. The reinforcement fabric used herein were supplied in rolls, with fabric being 1 m wide and 10 m long. Therefore, an overlap of roughly 152 mm was used to cover the full surface of the test panels (Fig. 2c). The selected overlap length of 152 mm was based on recommendations given in ACI 549-13 [8] and on the basis of manufacturer recommendations.



Fig. 2 – Photos of FRCM strengthening application

### 3.4 Test Setup

Two different types of test setup were used to investigate the in plane diagonal shear strength in accordance with ASTM E519-15 standard test guidelines [36]. The test procedure allows inducing a diagonal shear cracking and/or bed joint sliding failure mode. The test panel was subjected to a gradually increasing monotonic loading under a displacement rate of 0.01 mm/s along the diagonal joining the opposite ends of the test panels using a 500 kN automated actuator. Applied diagonal force was measure using a 500 kN load cell and corresponding displacements along both the diagonals of the test panel were recorded using four linear variable displacement transducers (LVDTs) mounted onto specially manufactured sliding guides with a gauge length of about 1200 mm. The LVDTs were attached along both diagonals on both faces of the test panel. The test setup used is shown in Fig. 3a. The FRCM strengthened specimens tilted out of plan at large loading magnitudes when tested in diagonal orientation and moved the hydraulic actuator outwards, which was owing to the localised crushing at loading shoes. Therefore, to achieve the ultimate failure load, the test setup was modified to test the FRCM strengthened specimens. In the modified test setup, load was applied manually using a hydraulic jack coupled with a 500 kN load cell. The applied loading rate was manually controlled to a displacement rate of more or less 0.01 mm/s. The modified test setup adopted is shown in Fig. 3b. The applied diagonal force was measure using the load cell coupled with the hydraulic jack and the resulting deformations along both the diagonals of the test panel were recorded using four draw-wire type linear displacement transducers (LDTs) mounted directly onto the specimen along both the diagonal with a gauge length of 1200 mm.



(a) Test setup for As-built specimen

(b) Test setup for strengthened specimens

Fig. 3 – Diagonal tensile test setup details



Table 5 – Diagonal shear testing results

S. No	Test panel	P <sub>max</sub> kN	v <sub>max</sub> MPa	v <sub>max</sub> /v <sub>0</sub>	ε <sub>y</sub> (×10 <sup>-3</sup> mm/mm)	ε <sub>u</sub> (×10 <sup>-3</sup> mm/mm)	μ	G GPa	E GPa	Observed failure mode
1	WA1	114	0.50	-	0.14	0.14	1.00	3.52	8.8	SJS
2	WG2	310	1.24	2.48	0.05	0.68	12.75	19.93	49.8	SM, LTC, TDC
3	WB3	336	1.34	2.68	0.11	0.99	9.00	13.6	34.2	SM, TDC, LTC
4	WB4	346	1.36	2.72	0.09	1.12	12.04	12.78	31.9	LTC, TDC
5	WG5	311	1.22	2.44	0.06	0.72	11.25	16.9	42.3	LTC, TDC, DB, SM
6	WC6	327	1.28	2.56	0.05	0.85	16.03	12.7	31.9	LTC, TDC
7	WC7	180	0.92	1.84	0.04	0.84	19.09	17.4	43.5	LTC, SM

Where: P<sub>max</sub> = maximum applied diagonal force; v<sub>max</sub> = maximum shear stress; ε<sub>y</sub> = shear strain at yield; ε<sub>u</sub> = shear strain at failure (corresponding to 0.80v<sub>max</sub>); μ = pseudo-ductility, (μ = ε<sub>u</sub>/ε<sub>y</sub>); G = modulus of rigidity; E = modulus of elasticity; v<sub>max</sub>/v<sub>0</sub> = ratio of the shear strength of strengthened wall panels (v<sub>max</sub>) to that of the as-built test panels (v<sub>0</sub>); SJS = step joint sliding; LTC = localized toe crushing; SM = splitting of concrete masonry units; TDC = TRM diagonal cracking and DB = debonding of FRCM.

#### 4. Experimental Results and Discussion

A summary of test results is given in Table 5. Shear strength of tested panels were calculated using Equation 1, where v<sub>max</sub> is the maximum recorded shear stress on net area, P<sub>max</sub> is the maximum recorded applied force, and A<sub>n</sub> is the net shear plane area of test panels in mm<sup>2</sup> calculated using Equation 2, w = width of specimen, h = height of specimen, and t = total thickness of specimen. The reported maximum shear strength values observed for all FRCM strengthened test panels were also expressed as ratio to the shear strength of the corresponding as-built test panel.

$$v_{max} = \frac{0.707 P_{max}}{A_n} \quad (1)$$

$$A_n = \frac{(w + h)t}{2} \quad (2)$$

##### 4.1 Crack patterns

The observed failure mode during the testing of as-built panel are shown in Fig. 4a. The as-built tested panel (WA1) performed with an approximately linear behaviour up to first cracking and then failed suddenly in a brittle manner, exhibiting bed joint sliding failure mode. As the applied tensile stresses reached the tensile strength of mortar-brick interface, which was mainly derived from cohesion in this case cracks propagated through the interface that lead to sudden collapse in a brittle manner.

On the contrary, a more ductile and gradual failure was exhibited by the FRCM strengthened specimens. First diagonal crack appeared at a load of 300 kN in specimen WG2, where diagonal cracking initiated along the line of action of applied force. The cracked initiated from the loaded corners and propagated towards the middle region of the test panel, followed by localised toe crushing and splitting of concrete masonry near the loading corners as shown in Fig. 4b. Test panel WB3 exhibited similar failure mode, with first diagonal crack appeared at a load of 309 kN that was followed toe crushing and concrete masonry splitting near the loaded corners. In specimen WB4 (see Fig. 4c) failure initiated with localised toe crushing at a load of 191 kN, whereas the diagonal crack appeared at 345 KN load. Localised damage in outer layer of the FRCM matrix was observed after diagonal cracking but the splitting of masonry was not observed. In specimen WG5, toe crushing started at a load of 296 kN and first crack appeared at 311 kN (see Fig. 4d), followed by vertical splitting of masonry units.



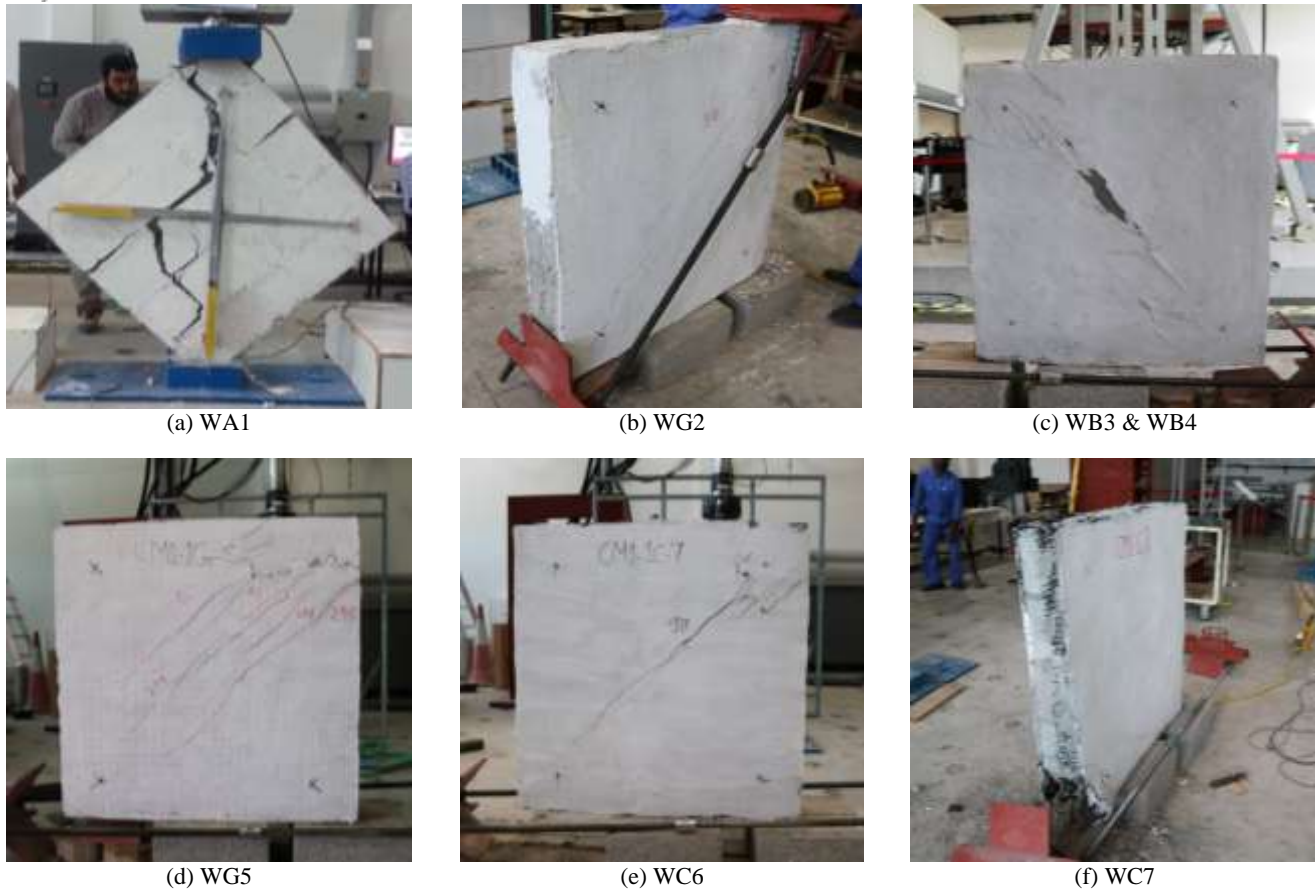


Fig. 4 – Observed crack patterns at the conclusion of tests

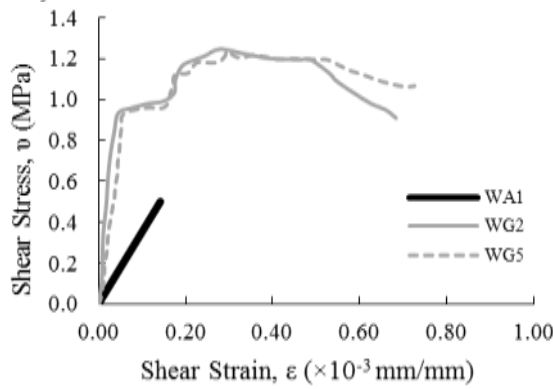
In specimen WC6 (see Fig. 4e), toe crushing started at a load of 170 kN and the diagonal first crack was noted at a load of 317 kN. The diagonal crack penetrating throughout the thickness of the FRCM matrix were observed, whereas the carbon fibre was not ruptured. Diagonal cracking was not observed in specimen WC7 because of the early toe crushing at one of the loaded ends at a load magnitude of 215 kN, which initiated masonry splitting (see Fig. 4f).

#### 4.2 Shear stress-strain response

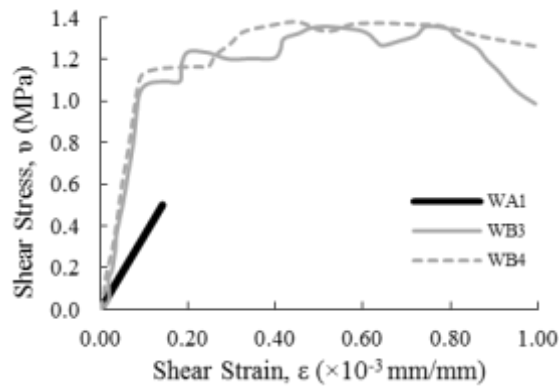
The experimentally measured diagonal force ( $P$ ) was transformed into shear stress ( $v$ ) using Equation 3. Where  $A_n$  is given by Equation 2. Measured strain values ( $\epsilon$ ) were calculated using Equation 4, where  $\Delta_s$  is diagonal shortening along the axis of applied force,  $\Delta_L$  is diagonal elongation measured perpendicular to the axis of applied force, and  $g$  is the gauge length of the displacement transducer.

$$v = \frac{0.707P}{A_n} \quad (3)$$

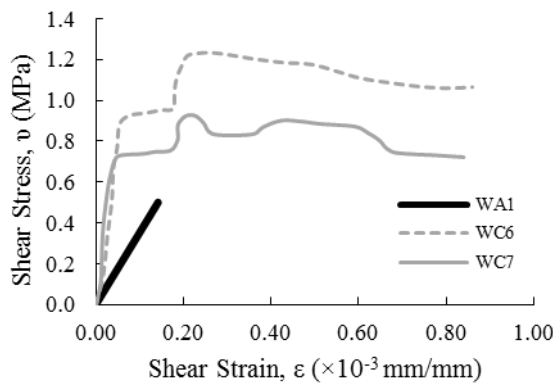
$$\epsilon = \frac{(\Delta_s + \Delta_L)}{2g} \quad (4)$$



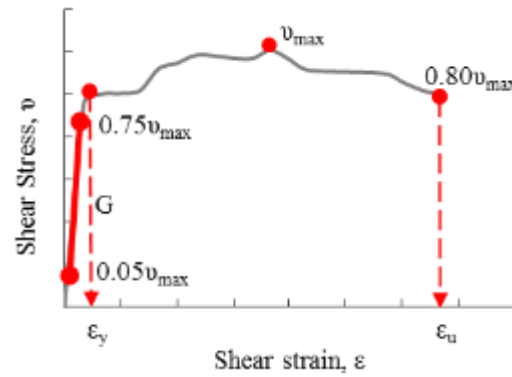
(a) WG2 and WG5



(b) WB3 and WB4



(c) WC6 and WC7



(d) Typical stress-strain behaviour

Fig. 6 – Experimental shear stress-strain response

Figs. 6a to 6c show the shear stress-strain ( $v$ - $\epsilon$ ) curves of tested wall panels, whereas Fig 6d shown the definition of reported parameters. In general, the  $v$ - $\epsilon$  curve of the as-built tested panel consisted of a linear initial portion until it suddenly collapsed/failed, with a sudden vertical drop in stress magnitude. FRCM strengthened test panels exhibited a linear-elastic behaviour up to cracking (characterised by the initial linear portion of the  $v$ - $\epsilon$  curves) and then a ductile failure mode with gradual decrease in the post-peak strength (characterised by flattened horizontal portion of the  $v$ - $\epsilon$  curves). Specimens retrofitted by glass and basalt FRCM have shown the same behaviour, whereas the specimens strengthened with carbon FRCM did not show same stress-strain curve because of the pre-mature localised corner crushing observed in wall panel WC7.

#### 4.4 Pseudo-ductility

Ductility is an important and desirable mechanical material property for the seismic resistance of structures. It represents the ability of a material/structural element to deform in-elastically after passing the maximum strength without failure. A structure having large ductility value would mean that the structure has the ability to yield and deform in-elastically without experiencing a significant loss of strength. The yield strain ( $\epsilon_y$ ) was determined from the stress-strain curves as the last point of the linear portion of the curve. The ultimate strain ( $\epsilon_u$ ) was determined as the strain value when the shear strength of the test panel degraded to  $0.80v_{max}$ . The values of ultimate and yield strain and the pseudo-ductility ( $\mu$ ) values determined using Equation 5 are reported in Table 5.

$$\mu = \frac{\epsilon_u}{\epsilon_y} \quad (5)$$



Pseudo-ductility is often used to generate capacity curve in displacement based design [37]. Referring to Table 5, it is noted that the ductility factor was determined corresponding to an induced diagonal failure mode and is highly sensitive to the calculated yield strain,  $\epsilon_y$ , which for the current tests showed considerable variability.

#### 4.5 Stiffness

The modulus of rigidity ( $G$ ) was determined as the secant modulus between the points corresponding to shear stress values of  $0.05\sigma_{max}$  and  $0.75\sigma_{max}$  of the shear stress-strain plots. The stiffness of test panels was quantified by the elastic modulus ( $E$ ), which were calculated using Equation 6 [38]. Values of the moduli for each tested panel are reported in Table 5.

$$E = 2G(1 + \nu) \quad (6)$$

Where:  $G$  = shear modulus, and  $\nu$  = poisson's ratio set to 0.25. The strengthened test panels showed an elastic modulus larger than their counterpart non-strengthened test panels.

## 5. Conclusions

The in-plane shear behaviour of FRCM strengthened IMPs was investigated by undertaking an experimental program, involving diagonal shear testing of seven masonry test panels. The effectiveness of FRCM strengthening schemes to limit damage to IMPs was evaluated. The preliminary results presented herein are part of a larger project investigating the effectiveness of different FRCM systems (i.e. cementitious matrices with GFRP, Basalt, and CFRP fabrics) to strengthen seismic deficient infilled concrete frames. Parameters pertaining to the seismic behaviour of in plane loaded IMPs were investigated and reported, which included shear stress-strain behaviour, shear strength, pseudo-ductility, and shear modulus. Test results from FRCM strengthened test panels were compared to those from a corresponding as-built tested panel and improvement in shear strength and deformation capacity was evaluated. The following are the key findings of the experimental program.

1. As usually is the case with unreinforced masonry, the as-built tested masonry panel underwent brittle failure and exhibited bed joints sliding failure mode. On the contrary, FRCM strengthened specimens behaved in a more ductile manner, with more gradual damage propagation through the FRCM layers along the loading diagonal.
2. Over all, shear strength increment due to FRCM strengthening ranged between 180-270% of that of as-built tested panel. The FRCM strengthened test panels did not collapse and neither the fabric rupture was observed. The failure mode of strengthened test panels was characterised by damage in localised regions (toes or middle diagonal region) and thus reported values are representative of the lower bound strength.
3. FRCM de-bonding from the substrate masonry was not observed at the conclusion of any tests reported herein, except localised bulging of fabrics at the loaded corners in some cases. This confirmed the efficiency of matrix-masonry interface strength and thus eliminating the need to use additional anchors. The failure of FRCM along the loaded diagonal was initiated due to slippage of fabric rovings inside the matrix, indicating that the fabric-matrix interface is the weakest link in the system.
4. Toe crushing was mostly the case with strengthened specimens, with crushing first starting at masonry toes followed by the vertical cracks propagation through the masonry units.
5. Nevertheless, FRCM was effective in increasing the shear strength and the deformation capacity of masonry panels and presents a potentially viable solution to improve the seismic performance of IMPs. However, this conclusions is pre-mature given the dataset is not yet comprehensive.

## 6. Acknowledgements

This study was funded by United Arab Emirates University under research grant G00001603. Engr. Tarek Salah, Mr. Faisal Abdulwahab, and Engr. Abdelrahman Alsallamin are thanked for their help with the test setup.



## 7. References

1. Kam W Y, Pampanin S. (2011): The seismic performance of RC buildings in the 22 February 2011 Christchurch earthquake. *Structural Concrete*, **12**(4): p. 223-233.
2. EERI. (2010): The Mw 8.8 Chile earthquake of February 27, 2010. *EERI Special Earthquake Report*.
3. Ismail N, Khattak N. (2015): *Reconnaissance report on the Mw 7.5 Hindu Kush earthquake of 26th October 2015 and the subsequent aftershocks*. United Arab Emirates University, Al Ain, UAE 2015; Available from: <https://www.eeri.org/2015/10/afghanistan-earthquake/>.
4. Ismail N, McGrannachan K, Hazelton G. (2013): Characterisation and seismic vulnerability assessment of unreinforced masonry buildings in Dunedin CBD. *Bulletin of The New Zealand Society for Earthquake Engineering*, **46**(3).
5. Kodur V, Bisby L, Green M. (2007): Preliminary guidance for the design of FRP-strengthened concrete members exposed to fire. *Journal of Fire Protection Engineering*, **17**(1): p. 5-26.
6. ACI-Committee-440. (2010): Guide for the design and construction of externally bonded fiber-reinforced polymer systems for strengthening unreinforced masonry structures. **ACI 440.7R-10**. American Concrete Institute 38800 Country Club Drive Farmington Hills, MI 48331.
7. Bisby L, Stratford T, Smith J, Halpin S. (2010): Comparative performance of fibre reinforced polymer and fibre reinforced cementitious mortar strengthening systems in elevated temperature service environments. in *Structural Faults and Repair*. Edingburgh, United Kingdom: Engineering Technics Press.
8. ACI-549.4-13. (2013): Guide to design and construction of externally bonded fabric-Reinforced Cementitious Matrix (FRCM) systems for repair and strengthening concrete and masonry structures. American Concrete Institute.
9. Koutas L, Bousias S, Triantafillou T. (2014): Seismic strengthening of masonry-infilled RC frames with TRM: Experimental study. *Journal of Composites for Construction*, **19**(2): p. 04014048.
10. Da Porto F, Guidi G, Verlato N, Modena C. (2015): Effectiveness of plasters and textile reinforced mortars for strengthening clay masonry infill walls subjected to combined in-plane/out-of-plane actions / Wirksamkeit von Putz und textilbewehrtem Mörtel bei der Verstärkung von Ausfachungswänden aus Ziegelmauerwerk, die kombinierter Scheiben- und Plattenbeanspruchung ausgesetzt sind. *Mauerwerk*, **19**(5): p. 334-354.
11. Selim M, Okten C, Ozkan M, Gencoglu. (2015): Behavior of RC frames with infill walls strengthened by cement based composites. in *The Twenty-fifth International Offshore and Polar Engineering Conference*. Hawaii, USA: International Society of Offshore and Polar Engineers.
12. Kolsch H. (1998): Carbon Fiber Cement Matrix (CFCM) overlay system for masonry strengthening. *Journal of Composites for Construction*, **2**(2): p. 105-109.
13. Papanicolaou C G, Triantafillou T C, Papathanasiou M, Karlos K. (2007): Textile reinforced mortar (TRM) versus FRP as strengthening material of URM walls: out-of-plane cyclic loading. *Materials and Structures*, **41**(1): p. 143-157.
14. Harajli M, ElKhatib H, San-Jose J. (2010): Static and cyclic out-of-plane response of masonry walls strengthened using textile-mortar system. *Journal of Materials in Civil Engineering*, **22**(11): p. 1171-1180.
15. Papanicolaou C, Triantafillou T, Lekka M. (2011): Externally bonded grids as strengthening and seismic retrofitting materials of masonry panels. *Construction and Building Materials*, **25**(2): p. 504-514.
16. Babaeidarabad S, Caso F, Nanni A. (2013): Out-of-Plane Behavior of URM Walls Strengthened with Fabric-Reinforced Cementitious Matrix Composite. *Journal of Composites for Construction*, **18**(4): p. 04013057.
17. Mantegazza G. (2006): Retrofitting concrete and masonry building: FRCM (fiber reinforced cementitious matrix) a new emerging technology. *XII Konferencja Naukowo-Techniczna Problemy Remontowe W Budownictwie Ogólnym i Obiektach Zabytkowych REMO*: p. 6-8.
18. Yardim Y, Lalaj O. (2016): Shear strengthening of unreinforced masonry wall with different fiber reinforced mortar jacketing. *Construction and Building Materials*, **102**: p. 149-154.
19. Ismail N, Ingham J M. (2014): Polymer textiles as a retrofit material for masonry walls. *Proceedings of the Institution of Civil Engineers - Structures and Buildings*, **167**(1): p. 15-25.
20. Almeida J A, Pereira E B, Barros J A. (2015): Assessment of overlay masonry strengthening system under in-plane monotonic and cyclic loading using the diagonal tensile test. *Construction and Building Materials*, **94**: p. 851-865.
21. Babaeidarabad S, Arboleda D, Loreto G, Nanni A. (2014): Shear strengthening of un-reinforced concrete masonry walls with fabric-reinforced-cementitious-matrix. *Construction and Building Materials*, **65**: p. 243-253.
22. Babaeidarabad S, De Caso F, Nanni A. (2013): URM walls strengthened with fabric-reinforced cementitious matrix composite subjected to diagonal compression. *Journal of Composites for Construction*, **18**(2): p. 04013045.
23. Basili M, Marcari G, Vestroni F. (2016): Nonlinear analysis of masonry panels strengthened with textile reinforced mortar. *Engineering Structures*, **113**: p. 245-258.



24. Faella C, Martinelli E, Nigro E, Paciello S. (2010): Shear capacity of masonry walls externally strengthened by a cement-based composite material: an experimental campaign. *Construction and Building Materials*, **24**(1): p. 84-93.
25. Parisi F, Iovinella I, Balsamo A, Augenti N, Prota A. (2013): In-plane behaviour of tuff masonry strengthened with inorganic matrix-grid composites. *Composites Part B: Engineering*, **45**(1): p. 1657-1666.
26. De Lorenzis L, Galati N, Ombres L. (2004): In-plane shear strengthening of natural masonry walls with NSM CFRP strips and FRCM overlay. in *Structural Analysis of Historical Constructions-2 Volume Set: Possibilities of Numerical and Experimental Techniques-Proceedings of the IVth Int. Seminar on Structural Analysis of Historical Constructions, 10-13 November 2004, Padova, Italy*. CRC Press.
27. Koutas L, Triantafillou T, Bousias S. (2014): Analytical modeling of masonry-infilled RC frames retrofitted with textile-reinforced mortar. *Journal of Composites for Construction*, **19**(5): p. 264-271.
28. Bernat E, Gil L, Roca P, Escrig C. (2013): Experimental and analytical study of TRM strengthened brickwork walls under eccentric compressive loading. *Construction and Building Materials*, **44**: p. 35-47.
29. Valluzzi M R, Da Porto F, Garbin E, Panizza M. (2014): Out-of-plane behaviour of infill masonry panels strengthened with composite materials. *Materials and Structures*, **47**(12): p. 2131-2145.
30. Bernat-Maso E, Escrig C, Aranha C A, Gil L. (2014): Experimental assessment of textile reinforced sprayed mortar strengthening system for brickwork wallettes. *Construction and Building Materials*, **50**: p. 226-236.
31. Ismail N, Ingham J M. (2016): In-plane and out-of-plane testing of unreinforced masonry walls strengthened using polymer textile reinforced mortar. *Engineering Structures*, **118**: p. 167-177.
32. ASTM-C109/C109M, Standard test method for compressive strength of hydraulic cement mortars (using 2-in. Or 50-mm cube specimens), in ASTM International, West Conshohocken PA. 2008.
33. ASTM-Committee-C270-03. (2003): Standard test method for compressive strength of masonry prisms. American Society for Testing and Materials International.
34. MSJC. (2011): Building code requirements for masonry structures (TMS 402-11/ACI 530-11/ASCE 5-11). *The Masonry Society, Boulder, CO*.
35. CEN. (2004): Eurocode 6: Design of masonry structures-Part 1-1: Common rules for reinforced and unreinforced masonry structures. *ENV 1996-1-1: 2004*.
36. ASTM-E519/E519M, ASTM E519: 2015. Standard test method for diagonal tension (shear) in masonry assemblages. 2015, PA: ASTM West Conshohocken.
37. Chopra A K, Goel R K. (1999): Capacity-demand-diagram methods based on inelastic design spectrum. *Earthquake spectra*, **15**(4): p. 637-656.
38. Ismail N, Petersen R B, Masia M J, Ingham J M. (2011): Diagonal shear behaviour of unreinforced masonry wallettes strengthened using twisted steel bars. *Construction and Building Materials*, **25**(12): p. 4386-4393.